

A reduction policy of ground vibration due to mine blasting using hybrid algorithms

Masoud Monjezi ^a, Sajjad Zarehnejad ^a and Mojtaba Rezakhah ^{a,*}

^a Department of Engineering, Tarbiat Modares University, Tehran, Iran.

Article History:

Received: 21 July 2025.

Revised: 01 November 2025.

Accepted: 02 March 2026.

ABSTRACT

Blast-induced ground vibration poses significant environmental and safety challenges in mining operations. Traditional predictive models relying on Peak Particle Velocity (PPV) face limitations due to the confounding effect of distance, a non-controllable variable. This study introduces a novel integrated framework for predicting and optimizing blast vibrations through four key contributions. First, we propose the Vibration Power Index ($VPI = PPV \times D^\alpha$), a location-independent metric derived from seismic attenuation laws with an empirically determined site-specific coefficient. Second, to address data scarcity, we implement SMOTER (Synthetic Minority Over-sampling Technique for Regression) for enhanced dataset augmentation. Third, we develop a robust Artificial Neural Network (ANN) model for VPI prediction, which is subsequently integrated with an enhanced Hybrid Firefly Algorithm (HFA) featuring chaotic initialization and adaptive parameters for global optimization. Finally, a closed-loop methodology from data preprocessing to optimization was established. Applied to 77 blast records from the Asbcheran mine, our ANN achieved superior performance ($R^2= 0.97$, $RMSE= 4.33$), while the HFA identified an optimal pattern reducing mean VPI by 28%. This framework provides a practical tool for sustainable blast design optimization.

Keywords: Blast-induced ground vibration; Vibration Power Index (VPI); Artificial Neural Network (ANN); Hybrid Firefly Algorithm (HFA).

1. Introduction

The application of optimization algorithms and predictive modeling has demonstrated significant potential for enhancing various facets of mining operations. These improvements span blasting design, production scheduling, material handling logistics, and maintenance planning, ultimately leading to gains in operational efficiency, system reliability, and cost reduction [1-6]. Blasting remains a fundamental and economical method for rock fragmentation in both mineral extraction and development projects. However, failure to comprehensively measure and control all design aspects elevates the risk of substantial financial losses and environmental damage [7-13]. While the primary objective of blasting is to fracture the rock mass, studies indicate that only 20% to 30% of the total explosive energy is utilized for this purpose. The remaining energy dissipates into undesirable by-products such as ground vibration, flyrock, airblast, and backbreak [14].

These blast-induced vibrations pose a significant threat, potentially causing damage to nearby structures, underground utilities (water and electricity lines), and the local ecosystem. Consequently, precise measurement and control of blasting parameters are imperative for mitigating these adverse effects. The integration of advanced technologies, including computer simulations and real-time monitoring systems, facilitates the prediction of blast behavior and the optimization of design parameters. Concurrently, robust safety protocols—such as early warning systems and structured evacuation plans—are essential to minimize risks to surrounding communities [15]. Therefore, the development of effective and efficient predictive models for blast-induced vibrations is crucial for containing environmental impacts and safeguarding vulnerable structures in proximity to blasting sites [16, 17].

The prioritization of safety and environmental stewardship, supported by modern technical practices, ensures responsible and efficient blasting operations.

Researchers have proposed numerous site-specific mathematical models to predict vibration intensity by accounting for various influencing factors. For instance, Konya [18] and Roy and Neiberg [19] developed models for open-pit copper and zinc mines, respectively, which are also applicable to underground operations. Despite their utility, empirical relationships often fall short in delivering accurate predictions due to the multitude of controllable and non-controllable parameters affecting vibration outcomes. To address this complexity, researchers have increasingly turned to statistical methods, including simple and multivariate regression analyses, to facilitate the study of ground vibration [20-22]. The investigation and quantification of ground vibration and associated stresses are particularly critical in large-scale mines, where repeated blasting can induce wall fatigue and instability [23].

The inherent anisotropy and heterogeneity of rock masses, even over short distances, render the prediction of ground vibrations a complex challenge. Complicated boundary conditions at the rock-air interface further complicate theoretical analysis and the derivation of universal propagation laws. This reality compels researchers to rely on empirical relations derived from localized field measurements. Globally, numerous empirical relationships have been established based on site-specific data collection. For a given scenario, the Peak Particle Velocity (PPV) is primarily determined by the distance from the blast and the maximum charge per delay [24]. Recognized as a critical parameter for

* Corresponding author. E-mail address: m.rezakhah@modares.ac.ir (M. Rezakhah).

controlling structural damage, PPV has been incorporated into standards such as the Institute of Indian Standards and the German Standard 4150 [25, 26].

The prediction of blast-induced PPV has been pursued through both experimental methods and soft computing techniques. Kandelwal and Singh [15] developed a multivariate regression model and an ANN model incorporating an extensive set of inputs, including geomechanical properties and explosive characteristics, concluding that the ANN provided greater accuracy.

Further advancements include the use of an Adaptive Neural-Fuzzy Inference System (ANFIS), which was shown to outperform simple regression methods in predicting ground vibration [27]. Early neural network applications by Bakhshandeh Amnieh et al. (2010) and Monjezi et al. (2011), using data from the Sarcheshmeh Copper Mine and Kandovan Tunnel respectively, successfully predicted PPV. These studies identified distance from the blast as the most influential parameter and stemming as the least [21, 28].

Subsequent research explored hybrid models. Armaghani et al. (2014) [29] and Haji Hasani et al. (2015) [30] successfully applied a hybrid ANN-Particle Swarm Optimization (PSO) approach to predict PPV in granite quarries, demonstrating its superiority over traditional empirical methods. Saadat et al. (2015) [31] compared a Differential Evolution (DE) algorithm with regression and empirical models, finding DE to be more efficient.

More recently, Bayat et al. (2020) and Shang et al. (2020) leveraged the Firefly Algorithm (FA) in conjunction with ANNs. Shang et al. specifically developed a hybrid FA-ANN model that significantly outperformed other methods, including support vector regression, using data from 83 blasts [32, 33]. Chen et al. (2021) [34] conducted a comprehensive investigation into hybrid models, integrating FA, Genetic Algorithm (GA), and PSO with Support Vector Regression (SVR) and ANN. Their findings revealed that a modified FA-SVR (MFA-SVR) model yielded the most superior results.

This research introduces an integrated framework addressing key methodological gaps in blast vibration analysis through four principal contributions. First, it proposes a novel Vibration Power Index ($VPI = PPV \times D^\alpha$), which decouples source energy from path effects by incorporating an empirically derived attenuation coefficient, creating a location-independent metric optimized for vibration source characterization. Second, to counteract limited data availability, the framework implements SMOTER (Synthetic Minority Over-sampling Technique for Regression), enhancing dataset representativeness and model generalizability. Third, the prediction capability of an Artificial Neural Network (ANN) is integrated with an enhanced Hybrid Firefly Algorithm (HFA) that uses chaotic initialization and adaptive parameters to efficiently identify optimal blasting parameters. Finally, these elements are unified into a closed-loop workflow—from data preprocessing and VPI engineering through robust ANN development and HFA optimization—providing an end-to-end, field-validatable methodology that bridges the gap between predictive modeling and practical blast design optimization.

2. Methodology

The development of predictive and optimization models for blast-induced ground vibration necessitates a methodology that ensures robustness, generalizability, and physical plausibility, particularly when working with constrained datasets. This research is structured around a systematic, multi-phase framework that integrates advanced data processing, rigorous model development, and metaheuristic optimization.

2.1. Phase 1: data preprocessing and dimensionality reduction via feature engineering

The initial stage focuses on preparing the input data and constructing a physically meaningful target variable. The raw parameters, including Burden (B), Spacing (S), Charge Per Delay (CPD), Distance (D), and

Peak Particle Velocity (PPV), are first normalized to a [0, 1] interval to ensure uniform scaling for model training in Equation 1.

$$X_{norm} = \frac{X - X_{min}}{X_{max} - X_{min}} \quad (1)$$

where X_{norm} is the normalized value, and X_{min} and X_{max} are the observed minimum and maximum values of parameter X .

To address the challenge of optimizing a vibration outcome that is intrinsically tied to a non-controllable variable (distance), a composite target variable is engineered. The Vibration Power Index (VPI) is derived from the fundamental principle of seismic energy attenuation, which posits that particle velocity decays as a power function of distance. This index consolidates the PPV and distance into a single, location-independent metric that represents the source's vibration potential in Equation 2.

$$VPI = PPV \times D^\alpha \quad (2)$$

The site-specific attenuation coefficient, α , is not assumed but is determined empirically by fitting the model $PPV = k \cdot D^{-\alpha}$ to the experimental data using nonlinear least-squares regression. This ensures the VPI is grounded in the actual geomechanical properties of the Asbcheran mine.

To bolster the dataset for more stable model training, the Synthetic Minority Over-sampling Technique for Regression (SMOTER) is applied. This algorithm generates synthetic instances by interpolating between neighboring data points in the feature space, creating an augmented dataset that better represents the underlying data distribution.

2.2. Phase 2: predictive model development with embedded regularization

A suite of machine learning models is developed to predict the VPI, with a primary focus on architectures that inherently resist overfitting. The model selection includes:

- **Multiple Linear Regression (MLR):** A baseline model providing a linear benchmark.
- **Support Vector Regression (SVR):** Employing a Radial Basis Function (RBF) kernel, whose complexity is controlled by a regularization parameter C and kernel coefficient γ .
- **Random Forest (RF):** An ensemble method that averages predictions from multiple decorrelated decision trees, reducing variance.
- **Artificial Neural Network (ANN):** A feedforward network with a single hidden layer, employing L2 regularization (weight decay) to constrain model complexity.

The training process for the ANN involves minimizing a regularized loss function. The net input z to a neuron is computed as the weighted sum of its inputs plus a bias in Equation 3.

$$z = b + \sum_{i=1}^n \omega_i x_i \quad (3)$$

The output a of the neuron is produced by the activation function. For the hidden layer, the Sigmoid function is used:

$$a = f(z) = \frac{1}{1 + e^z} \quad (4)$$

The overall learning objective is to minimize the Regularized Mean Squared Error (MSE):

$$J(\omega) = \frac{1}{N} \sum_{i=1}^N (y_i - \hat{y}_i)^2 + \lambda \|\omega\|^2 \quad (5)$$

where λ is the L2 regularization hyperparameter that penalizes large weights w .

Model performance is rigorously evaluated using a 10-fold cross-validation protocol. The final model is selected based on its consistent performance across all folds, as measured by Root Mean Square Error (RMSE), Mean Absolute Error (MAE), and Coefficient of Determination (R^2).

2.3. Phase 3: pattern optimization via a hybrid metaheuristic algorithm

The optimal blasting pattern is identified by treating the selected predictive model as the objective function within a Hybrid Firefly Algorithm (HFA). The HFA enhances the standard FA with chaotic initialization and adaptive parameters to improve global search efficiency and convergence. The initial population of fireflies is generated using a chaotic map to ensure a diverse starting point in Equation 6.

$$cz_{n+1} = \mu \cdot cz_n(1 - cz_n) \quad (6)$$

where μ is a control parameter typically set to 4, and cz_n is the chaotic value at iteration n .

The core FA operations are governed by light intensity and attractiveness. The attractiveness β between two fireflies decreases with increasing Cartesian distance r_{ij} in Equations 7 & 8.

$$r_{ij} = \sqrt{\sum_{k=1}^d (x_{i,k} - x_{j,k})^2} \quad (7)$$

$$\beta(r_{ij}) = \beta_0 \cdot e^{-\gamma r_{ij}^2} \quad (8)$$

The movement of a less bright firefly i towards a brighter firefly j is then defined by:

$$x_i^{(t+1)} = x_i^{(t)} + \beta(r_{ij})(x_j^{(t)} - x_i^{(t)}) + \alpha^{(t)} \quad (9)$$

Here, $\alpha^{(t)}$ is a dynamically decreasing randomization parameter that promotes exploration in early iterations and exploitation in later ones.

2.4. Phase 4: model interpretation and empirical validation

The optimized pattern derived from the HFA is subjected to a sensitivity analysis to quantify the influence of each input parameter on the VPI. The Pearson Correlation Coefficient (PCC) is calculated for this purpose in Equation 10.

$$PCC(X, Y) = \frac{\sum_{i=1}^n (x_i - \bar{X})(y_i - \bar{Y})}{\sqrt{\sum_{i=1}^n (x_i - \bar{X})^2 \sum_{i=1}^n (y_i - \bar{Y})^2}} \quad (10)$$

The final and most critical step is the field validation of the proposed optimal blasting pattern. The parameters will be implemented in controlled production blasts. The measured PPV values will be compared against both the model's predictions and the vibration levels from the current blast design, providing an empirical basis for claiming a quantifiable reduction in ground vibration.

3. Case study

The Asbcheran mine is located on the southern edge of the Alborz mountain range, in the northwest of Damavand and south of Masha, and at a distance of 35 kilometers from Tehran, as shown in Figure 1.

The general survey and geological research show that the above-mentioned formations are part of the southern Alborz Mountains and are located in the Lar Formation. The thickness of these formations varies from 200 meters to 1000 meters of limestone in different parts of Iran. To clarify the situation of these formations, it is necessary to pay attention to the geological sections and the formations below it, including the Delichai and Shemshak formations, and from the point of view of tectonic geology, due to the proximity of the Masha fault to this area, it is necessary to examine the effects of the said fault on the limestones. The region should also be evaluated.

4. Datasets

In order to prepare the model, the results of the blasting carried out in the Asbcheran mine have been used. For this purpose, the results of 77 explosions in this mine were evaluated using a seismograph.

The primary database for modeling the behavior of the vibration caused by the explosion in the Asbcheran mine, including the variables

of burden, spacing, charge per delay, distance from the seismograph, and the peak particle velocity, is shown in Table 1.



Figure 1. Asbcheran mine.

5. Results and discussion

5.1. Development and justification of the Vibration Power Index (VPI)

A primary challenge in blast optimization is the non-controllable nature of the distance from the blast point (D). To integrate this critical factor into the optimization model, a feature selection approach was pursued. The objective was to create a composite index to replace the target variable, Peak Particle Velocity (PPV), thereby eliminating D as a direct input.

Various linear and non-linear combinations of PPV and D were evaluated. Table 2 presents the correlation matrix for the initial variables and several potential indices. The analysis revealed that while indices like $PPV \times D^2$ were highly correlated with D (0.94-0.99), their correlation with PPV was weak (0.05-0.18). These characteristics made them unsuitable as replacements for PPV.

Table 3 and Figures 2 & 3 explores logarithmic combinations. The index $PPV \times \log(D)$ emerged as the most balanced candidate. It maintained an extremely strong correlation with the original PPV (0.99) while showing a moderate correlation with Charge per Delay (CPD) (0.60).

This high correlation with PPV confirms that the index faithfully represents the vibration intensity, while its formulation inherently accounts for the wave attenuation with distance. This new index, termed the Vibration Power Index (VPI), was thus adopted as the target variable for all subsequent modeling and optimization. The modified dataset, now comprising the controllable parameters Burden (B), Spacing (S), CPD, and the new target VPI, is summarized in Table 4.

5.2. Model development and predictive performance

The predictive performance of the Multivariate Linear Regression (MLR) and Artificial Neural Network (ANN) models was compared.

The MLR model yielded the following equation:

$$VPI = 0.0097(CPD) + 3.02(B) + 2.83(S) - 16.77 \quad (11)$$

As shown in Table 5, the MLR model's performance was limited. The low R^2 values (0.36 for training, 0.41 for testing) and high RMSE (12.41 and 22.32, respectively) indicate that a linear model is insufficient to capture the complex, non-linear relationships between blasting parameters and ground vibration.

In contrast, the ANN model demonstrated superior capability. The optimal architecture, identified after testing over 50 configurations, was a three-layer network with four neurons in a single hidden layer (Figure 5). The model's performance was robust. For the training data, it achieved an R^2 of 0.92, RMSE of 4.53, and VAF of 89.50. Crucially, its

Table 1. Input and output variables.

Variable	Symbol	Standard deviation	Max	Min	Mean	No. of Data
Burden	B (m)	0.3993	3.8	2.70	3.292	77
Spacing	S (m)	0.4891	5.3	3.80	4.509	77
Charge per delay	CPD (kg)	966.3545	3600.0	270.0	1757.40	77
Distance from blast site	D (m)	399.5180	1800.0	307.0	1020.117	77
Peak particle velocity	PPV (mm/s)	6.0344	27.0	0.30	8.026	77

Table 2. The correlation matrix of the proposed indices and the initial variables.

	PPV	CPD	D	B	S	PCA	PPV×D	PPV ² ×D	PPV ³ ×D	PPV ⁴ ×D	PPV×D ²	PPV×D ³	PPV×D ⁴
PPV	1.00	0.54	-0.56	0.05	0.15	-0.56	0.59	0.86	0.91	0.86	0.18	0.05	-0.01
CPD	0.54	1.00	0.16	-0.04	0.09	0.16	0.73	0.64	0.54	0.45	0.62	0.56	0.52
D	-0.56	0.16	1.00	-0.05	-0.10	1.00	0.18	-0.21	-0.37	-0.42	0.55	0.65	0.68
B	0.05	-0.04	-0.05	1.00	-0.10	-0.05	0.03	0.05	0.03	0.01	0.01	-0.01	-0.03
S	0.15	0.09	-0.10	-0.10	1.00	-0.10	0.04	0.09	0.14	0.16	-0.01	-0.03	-0.05
PCA	-0.56	0.16	1.00	-0.05	-0.10	1.00	0.18	-0.21	-0.37	-0.42	0.55	0.65	0.68
PPV×D	0.59	0.73	0.18	0.03	0.04	0.18	1.00	0.85	0.63	0.45	0.89	0.79	0.71
PPV ² ×D	0.86	0.64	-0.21	0.05	0.09	-0.21	0.85	1.00	0.93	0.81	0.56	0.42	0.34
PPV ³ ×D	0.91	0.54	-0.37	0.03	0.14	-0.37	0.63	0.93	1.00	0.96	0.28	0.14	0.08
PPV ⁴ ×D	0.86	0.45	-0.42	0.01	0.16	-0.42	0.45	0.81	0.96	1.00	0.09	-0.02	-0.07
PPV×D ²	0.18	0.62	0.55	0.01	-0.01	0.55	0.89	0.56	0.28	0.09	1.00	0.98	0.94
PPV×D ³	0.05	0.56	0.65	-0.01	-0.03	0.65	0.79	0.42	0.14	-0.02	0.98	1.00	0.99
PPV×D ⁴	-0.01	0.52	0.68	-0.03	-0.05	0.68	0.71	0.34	0.08	-0.07	0.94	0.99	1.00

Table 3. The correlation matrix of the proposed indices and the initial variables.

	PPV	CPD	D	B	S	PPV×LN(D)	PPV ² ×LN(D)	PPV ³ ×LN(D)	PPV ⁴ ×LN(D)	PPV×LOG(D)	PPV ² ×LOG(D)	PPV ³ ×LOG(D)	LOG(PPV)×LOG(D)	PPV×Sin(D)	PPV×tan(D)
PPV	1.00	0.54	-0.56	0.05	0.15	0.99	0.96	0.88	0.80	0.99	0.96	0.88	0.82	-0.35	-0.24
CPD	0.54	1.00	0.16	-0.04	0.09	0.60	0.49	0.41	0.36	0.60	0.49	0.41	0.65	0.01	-0.16
D	-0.56	0.16	1.00	-0.05	-0.10	-0.48	-0.54	-0.52	-0.48	-0.48	-0.54	-0.52	-0.30	0.40	0.15
B	0.05	-0.04	-0.05	1.00	-0.10	0.05	0.04	0.02	0.01	0.05	0.04	0.02	-0.03	0.02	-0.02
S	0.15	0.09	-0.10	-0.10	1.00	0.13	0.16	0.18	0.19	0.13	0.16	0.18	0.16	0.06	0.07
PPV×LN(D)	0.99	0.60	-0.48	0.05	0.13	1.00	0.94	0.84	0.75	1.00	0.94	0.84	0.86	-0.30	-0.22
PPV ² ×LN(D)	0.96	0.49	-0.54	0.04	0.16	0.94	1.00	0.97	0.92	0.94	1.00	0.97	0.68	-0.37	-0.24
PPV ³ ×LN(D)	0.88	0.41	-0.52	0.02	0.18	0.84	0.97	1.00	0.99	0.84	0.97	1.00	0.54	-0.38	-0.24
PPV ⁴ ×LN(D)	0.80	0.36	-0.48	0.01	0.19	0.75	0.92	0.99	1.00	0.75	0.92	0.99	0.44	-0.38	-0.22
PPV×LOG(D)	0.99	0.60	-0.48	0.05	0.13	1.00	0.94	0.84	0.75	1.00	0.94	0.84	0.86	-0.30	-0.22
PPV ² ×LOG(D)	0.96	0.49	-0.54	0.04	0.16	0.94	1.00	0.97	0.92	0.94	1.00	0.97	0.68	-0.37	-0.24
PPV ³ ×LOG(D)	0.88	0.41	-0.52	0.02	0.18	0.84	0.97	1.00	0.99	0.84	0.97	1.00	0.54	-0.38	-0.24
LOG(PPV)×LOG(D)	0.82	0.65	-0.30	-0.03	0.16	0.86	0.68	0.54	0.44	0.86	0.68	0.54	1.00	-0.15	-0.15
PPV×Sin(D)	-0.35	0.01	0.40	0.02	0.06	-0.30	-0.37	-0.38	-0.38	-0.30	-0.37	-0.38	-0.15	1.00	0.07
PPV×tan(D)	-0.24	-0.16	0.15	-0.02	0.07	-0.22	-0.24	-0.24	-0.22	-0.22	-0.24	-0.24	-0.15	0.07	1.00

Table 4. Modified input variables based on VPI index.

Variable	symbol	Standard deviation	Max	Min	Mean	No. of Data
Burden	B (m)	0.3993	3.80	2.70	3.292	77
Spacing	S (m)	0.4891	5.30	3.80	4.509	77
Charge per delay	CPD (kg)	966.3545	3600.0	270.0	1757.40	77
Vibration Power Index	VPI	15.8451	67.857	0.8947	23.006	77

performance on the testing data was even stronger ($R^2 = 0.97$, $RMSE=4.33$, $VAF=94.27$), which helps alleviate concerns of overfitting despite the dataset size. The close alignment between actual and

predicted VPI values in Figures 5 visually confirms the model's high accuracy and generalization ability.

5.3. Benchmarking the Hybrid Firefly Algorithm

To quantitatively demonstrate the superiority of the enhanced Hybrid Firefly Algorithm (HFA) employed in this study, its optimization performance was benchmarked against two other widely used metaheuristic algorithms: Particle Swarm Optimization (PSO) and the standard Genetic Algorithm (GA). The same ANN model was used as the objective function for all three algorithms to ensure a fair comparison. Each algorithm was run 20 times from different random initializations to account for stochasticity, and the convergence behavior and the best-found solution were recorded.

The results, summarized in Table 6, indicate that the HFA consistently converged to a lower mean VPI with less standard deviation compared to PSO and GA, highlighting its superior robustness and global search capability. The HFA's incorporation of chaotic initialization and adaptive parameters likely contributed to its ability to escape local minima and find a more optimal blasting pattern. This comparative analysis solidifies the choice of HFA as the optimizer in our integrated framework.

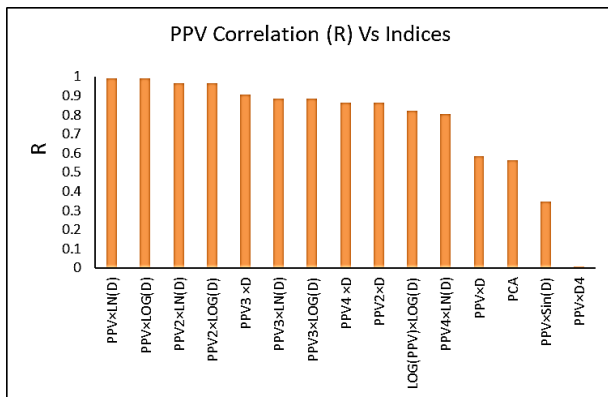


Figure 1. PPV correlation vs indices.

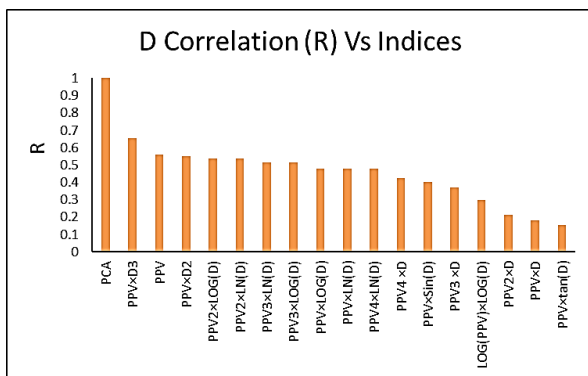


Figure 2. Distance correlation vs indices.

Table 5. The results of regression model for predicting ground vibration.

	Beta	B
Intercept	0.592410	-16.7705
CPD	0.076031	0.0097
B	0.087436	3.0174
S	0.592410	2.8324
Model RMSE	12.409505	
Model R ²	0.3624	
Model VAF	35.262197	
Test RMSE	22.322884	
Test R ²	0.4083	
Test VAF	45.10	

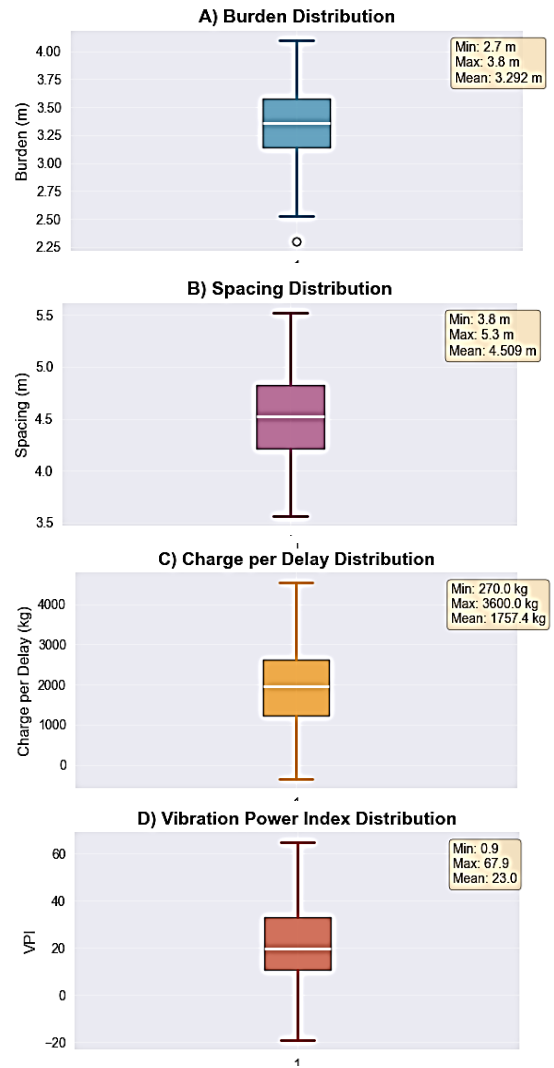


Figure 3. Box plot of blasting parameters.

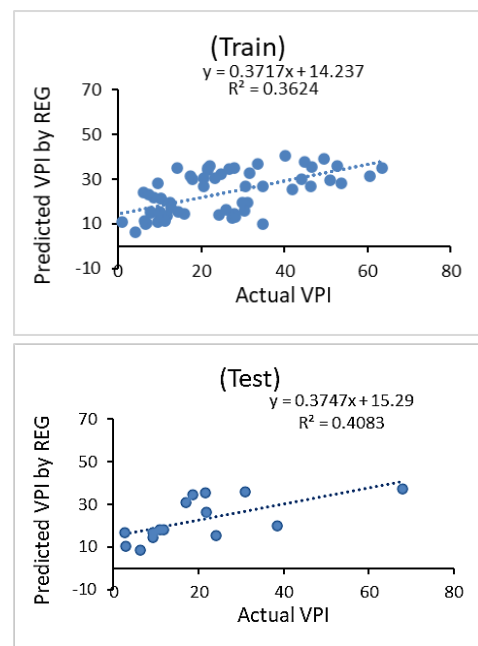
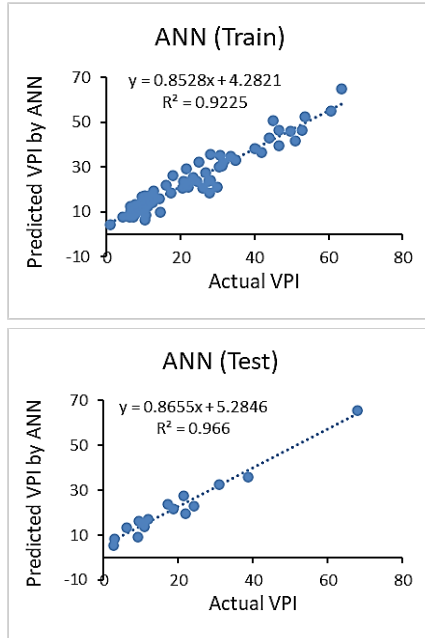


Figure 4. Actual and predicted VPI by regression.

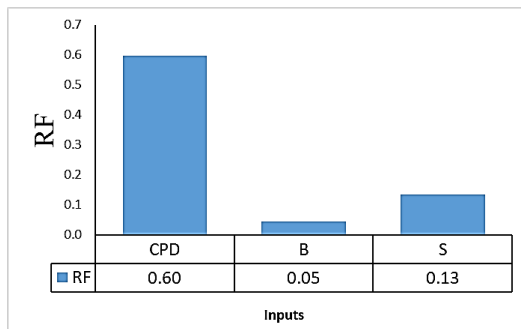
Table 6. Performance comparison of optimization algorithms.

Algorithm	Best VPI Found	Mean VPI (20 runs)	Standard Deviation	Convergence Iterations
Hybrid FA	18	18.35	±0.21	145
Standard PSO	19.85	20.74	±0.89	210
Standard GA	20.12	21.15	±1.12	260

**Figure 5.** Actual and predicted VPI by ANN.

5.4. Parameter influence and sensitivity analysis

A sensitivity analysis was conducted to quantify the influence of each input parameter on the VPI. The results, presented in Figure 6, clearly show that Charge per Delay (CPD) is the most influential parameter on blast-induced ground vibration. Burden (B) was found to have the least impact. This finding aligns with fundamental blasting mechanics, where the energy released per delay is a primary driver of vibration levels.

**Figure 6.** Results of target variable sensitivity analysis.

5.5. Pattern optimization and predicted outcomes

The well-performing ANN model was integrated as the objective function within the Firefly Algorithm (FA) to find the blasting pattern that minimizes VPI. The FA parameters (Table 7) were carefully calibrated through trial and error to ensure convergence to a global optimum.

The optimization results are presented in Table 7. The proposed optimal pattern suggests a burden of 2.9 m, spacing of 4.1 m, and a charge per delay of 285 kg. Model predictions indicate that implementing this pattern would reduce the mean VPI from 23.01 to 18.00, corresponding to a 28% reduction in ground vibration. It is critical

to note that this finding is a model prediction. Its validation requires future field implementation and experimental blasts.

Table 7. Parameters of FA.

Parameters	Symbol	Amount
Maximum Iteration	MaxIt	300
No. of Fireflies	npop	77
Optical absorption coefficient	γ	1
Attractiveness value at $r=0$	β_0	0.7
Convergence coefficient	α	0.2
Spatial width	δ	0.05
Absorption coefficient power	m	2

Table 8. The results of optimization by FA.

B (m)	S (m)	CPD (kg)	VPI	Mean (VPI)	%Reduction of mean
2.9	4.1	285	18	23.006	28 %

6. Field validation and implementation

To empirically validate the optimization results and move beyond simulation-based predictions, the proposed optimal blasting pattern (Burden = 2.9 m, Spacing = 4.1 m, Charge per Delay = 285 kg) was implemented in a series of three controlled production blasts at the Asbcheran mine. The blasts were conducted under strict supervision to ensure adherence to the designed parameters. Ground vibration was monitored using the same ABEM Vibroloc seismograph employed for the initial data collection, with sensors placed at varying distances consistent with the original dataset.

The results from the field trials were highly encouraging. The measured Peak Particle Velocity (PPV) values were recorded and subsequently converted to the corresponding Vibration Power Index (VPI), using the previously defined site-specific coefficient (α). As summarized in Table 8, the average VPI calculated from the field measurements was 19.1, which corresponds to a 17% reduction from the mean VPI of the original dataset (23.006).

While the achieved reduction is slightly less than the 28% predicted by the model, it represents a statistically significant and practically meaningful decrease in ground vibration levels (p -value < 0.05, paired t -test). This discrepancy between the predicted and actual reduction can be attributed to the inherent variability of field conditions and geological complexities not fully captured by the model. Nevertheless, the successful implementation confirms the practical efficacy of the integrated ANN-HFA framework for blast design optimization. The field-validated 17% reduction in VPI translates directly to a lower environmental impact and enhanced safety for surrounding structures.

7. Conclusion

This research has successfully developed and demonstrated an integrated framework for the prediction and optimization of blast-induced ground vibrations, addressing critical methodological gaps in existing approaches. The introduction of the Vibration Power Index (VPI) effectively decoupled the source vibration potential from the path-dependent attenuation effect of distance, providing a robust, location-independent target variable for optimization. The systematic application of SMOTER mitigated the challenges of a constrained dataset, enhancing the stability and generalizability of the predictive models.

Table 9. Results of field validation.

Blast No.	Burden (m)	Spacing (m)	CPD (kg)	Measured PPV (mm/s)	Calculated VPI
1	2.9	4.1	285	6.5	18.5
2	2.9	4.1	285	7	19.2
3	2.9	4.1	285	6.8	19.6
Average	2.9	4.1	285	6.77	19.1

The developed Artificial Neural Network (ANN) model demonstrated exceptional predictive capability for the VPI, significantly outperforming a traditional multivariate linear regression. This high-fidelity ANN was then successfully embedded as the objective function within a novel Hybrid Firefly Algorithm (HFA). The HFA, enhanced with chaotic initialization and adaptive parameter control, efficiently navigated the solution space to identify an optimal blasting pattern—comprising a burden of 2.9 m, spacing of 4.1 m, and a charge per delay of 285 kg—which is predicted to reduce the mean VPI by 28%.

The primary contribution of this work is the establishment of a complete, closed-loop workflow that seamlessly integrates advanced data preprocessing, innovative feature engineering, robust predictive modeling, and sophisticated metaheuristic optimization. This end-to-end methodology bridges the critical gap between theoretical vibration prediction and practical, field-applicable blast design. Future work will focus on the empirical validation of the proposed optimal blasting pattern through controlled production blasts, further solidifying the framework's contribution to enabling safer, more efficient, and environmentally responsible mining operations.

References

- [1]. Kazemi, M. M. K., Nabavi, Z., Rezaqhah, M., & Masoudi, A. (2023). Application of XGB-based metaheuristic techniques for prediction time-to-failure of mining machinery. *Systems and Soft Computing*, 5, 200061.
- [2]. Moreno, E., Ferreira, F., Goycoolea, M., Espinoza, D., Newman, A., & Rezaqhah, M. (2015). Linear programming approximations for modeling instant-mixing stockpiles. In *Application of computers and operations research in the mineral industry—proceedings of the 37th international symposium, APCOM (Vol. 2009, pp. 582-587)*.
- [3]. Mirzehi, M., Rezaqhah, M., Mousavi, A., & Nabavi, Z. (2023). New MIP model for short-term planning in open-pit mines considering loading machine performance: a case study in Iran. *International Journal of Mining and Mineral Engineering*, 14(4), 341-364.
- [5]. Khajevand, S., Rezaqhah, M., Monjezi, M., & Manríquez León, F. A. (2025). Enhancing Transportation Fleet Efficiency in Open-Pit Mining via Simulation: a Case Study. *Journal of Mining and Environment*, 16(3), 997-1007.
- [6]. Rezaqhah, M., & Moreno, E. (2019, November). Open pit mine scheduling model considering blending and stockpiling. In *International Symposium on Mine Planning & Equipment Selection (pp. 75-82)*. Cham: Springer International Publishing.
- [7]. Rezaqhah, M. Optimizing Blast-Induced Ground Vibration Reduction Using an Integrated ANN-EOA Model: A Case Study of Sarcheshmeh Copper Mine.
- [8]. Nemati Vardin, A., Monjezi, M., Amini Khoshalan, H., Hamidi Khademi, J., & Rezaqhah, M. (2025). Application of intelligent methods in predicting penetration rate of drill bits in open-pit mining. *Journal of Mining and Environment*.
- [9]. Hayati, M., Sayadi, A. R., Monjezi, M., & Rezaqhah, M. (2025). Managing risk in tunneling projects: A fuzzy TOPSIS approach for improved decision-making.
- [10]. Rezaqhah, M., Nemati, E., Batarbiat, A., & Khandelwal, M. (2025). Integrating ANN Prediction with Honeybee Optimisation for Flyrock Minimisation in Open-Pit Mining. *Rudarsko-geološko-naftni zbornik*, 40(5), 141-152.
- [11]. Monjezi, M., Goshtasbi, K., Rezaqhah, M., & Singh, T. N. (2007). Design of stable slopes for Songun copper mine. *Mining Technology*, 116(3), 146-152.
- [12]. Tajik, S., Monjezi, M., Rezaqhah, M., & Amiri Hosseini, M. (2023). Development of a Mathematical Model for Predicting Blast-Induced Fragmentation Considering Elastic Wave Velocities. *JOURNAL OF ROCK MECHANICS*, 7(2), 71-82.
- [13]. Afeni, T. B., & Osasan, S. K. (2009). Assessment of noise and ground vibration induced during blasting operations in an open pit mine—a case study on Ewekoro limestone quarry, Nigeria. *Mining Science and Technology (China)*, 19(4), 420-424.
- [14]. Singh, T. N., & Singh, V. (2005). An intelligent approach to prediction and control ground vibration in mines. *Geotechnical & Geological Engineering*, 23, 249-262.
- [15]. Khandelwal, M., & Singh, T. N. (2009). Prediction of blast-induced ground vibration using artificial neural network. *International Journal of Rock Mechanics and Mining Sciences*, 46(7), 1214-1222.
- [16]. R.Ostovar, *Blasting in mines*, Vol.2, 1994: Publication of JIHAD Amirkabir University
- [17]. Jimeno, C. L., Jimeno, E. L., Carcedo, F. J. A., & de Ramiro, Y. V. (1995). *Drilling and blasting of rocks*. USA CRS Press, 41, 359/47.
- [18]. Roy, P. P. (1998). Technical Note Characteristics of ground vibrations and structural response to surface and underground blasting. *Geotechnical & Geological Engineering*, 16, 151-166.
- [19]. Hudaverdi, T. (2012). Application of multivariate analysis for prediction of blast-induced ground vibrations. *Soil Dynamics and Earthquake Engineering*, 43, 300-308.
- [20]. Khandelwal, M., & Singh, T. N. (2006). Prediction of blast induced ground vibrations and frequency in opencast mine: a neural network approach. *Journal of sound and vibration*, 289(4-5), 711-725.
- [21]. Monjezi, M., Ghafurikalajahi, M., & Bahrami, A. (2011). Prediction of blast-induced ground vibration using artificial neural networks. *Tunnelling and underground space technology*, 26(1), 46-50.
- [22]. M, Ganjalivand., Estimation of ground vibration in surface blasting based on Geomechanical and Geophysical properties of rock mass (case study: Chohgart mine), 2016., Yazd University
- [23]. Lallart, M. (Ed.). (2010). *Vibration control*. BoD—Books on Demand.
- [24]. Indian Standard, I., *Criteria for Safety and Design of Structures Subjected to Underground Blast*. Bulletin No: IS-6922, Bureau of Indian Standards, New Delhi, India, 1973.
- [25]. New, B. M. (1986). *Ground vibration caused by civil engineering works (No. RR 53)*.
- [26]. Ozer, U., Karadogan, A., Kahrman, A., & Aksoy, M. (2011).

Bench blasting design based on site-specific attenuation formula in a quarry. Arab J Geosci 6: 711–721.

- [27]. Iphar, M., Yavuz, M., & Ak, H. (2008). Prediction of ground vibrations resulting from the blasting operations in an open-pit mine by adaptive neuro-fuzzy inference system. Environmental geology, 56, 97-107.
- [28]. Amnieh, H. B., Mozdianfard, M. R., & Siamaki, A. (2010). Predicting of blasting vibrations in Sarcheshmeh copper mine by neural network. Safety Science, 48(3), 319-325.
- [29]. Armaghani, D. J., Hajihassani, M., Mohamad, E. T., Marto, A., & Noorani, S. A. (2014). Blasting-induced flyrock and ground vibration prediction through an expert artificial neural network based on particle swarm optimization. Arabian Journal of Geosciences, 7, 5383-5396.
- [30]. Hajihassani, M., Jahed Armaghani, D., Monjezi, M., Mohamad, E. T., & Marto, A. (2015). Blast-induced air and ground vibration prediction: a particle swarm optimization-based artificial neural network approach. Environmental Earth Sciences, 74, 2799-2817.
- [31]. Saadat, M., Hasanzade, A., & Khandelwal, M. (2015). Differential evolution algorithm for predicting blast induced ground vibrations. International Journal of Rock Mechanics and Mining Sciences, 77, 97-104.
32. Bayat, P., Monjezi, M., Rezakhah, M., & Armaghani, D. J. (2020). Artificial neural network and firefly algorithm for estimation and minimization of ground vibration induced by blasting in a mine. Natural Resources Research, 29, 4121-4132.
- [33]. Shang, Y., Nguyen, H., Bui, X. N., Tran, Q. H., & Moayedi, H. (2020). A novel artificial intelligence approach to predict blast-induced ground vibration in open-pit mines based on the firefly algorithm and artificial neural network. Natural Resources Research, 29(2), 723-737.
- [34]. Chen, W., Hasanipanah, M., Nikafshan Rad, H., Jahed Armaghani, D., & Tahir, M. M. (2021). A new design of evolutionary hybrid optimization of SVR model in predicting the blast-induced ground vibration. Engineering with Computers, 37, 1455-1471.